Proteomic analysis of multiple primary cilia reveals a novel mode of ciliary development in mammals

Keishi Narita[1], Hiroko Kozuka-Hata[2], Yuta Nonami[3], Hiroko Ao-Kondo[2], Toshimitsu Suzuki[4], Hideki Nakamura[3], Kazuhiro Yamakawa[4], Masaaki Oyama[2], Takafumi Inoue[3] and Sen Takeda[1,*]

[1]Department of Anatomy and Cell Biology, Interdisciplinary Graduate School of Medicine and Engineering, University of Yamanashi, 1110 Shimo-Kateau, Chuo, Yamanashi 409-3898, Japan
[2]Medical Proteomics Laboratory, Institute of Medical Science, The University of Tokyo, 4-6-1 Shirokanedai, Minato-ku, Tokyo 108-8639, Japan
[3]Department of Life Science and Medical Bioscience, Waseda University, Shinjuku-ku, Tokyo 162-8480, Japan
[4]Laboratory for Neurogenetics, RIKEN Brain Science Institute, 2-1 Hirosawa, Wako, Saitama 351-0198, Japan
*Author for correspondence (stakeda@yamanashi.ac.jp)

Biology Open 1, 815–825
doi: 10.1242/bio.20121081
Received 28th February 2012
Accepted 21st May 2012

Summary

Cilia are structurally and functionally diverse organelles, whose malfunction leads to ciliopathies. While recent studies have uncovered common ciliary transport mechanisms, limited information is available on the proteome of cilia, particularly that of sensory subtypes, which could provide insight into their functional and developmental diversities. In the present study, we performed proteomic analysis of unique, multiple 9+0 cilia in choroid plexus epithelial cells (CPECs). The analysis of juvenile swine CPEC cilia identified 868 proteins. Among them, 396 were shared with the proteome of 9+0 photoreceptor cilia (outer segment), whereas only 152 were shared with the proteome of 9+2 cilia and flagella. Various signaling molecules were enriched in a CPEC-specific ciliome subset, implicating multiplicity of sensory functions. The ciliome also included molecules for ciliary motility such as Rsph9. In CPECs from juvenile swine or adult mouse, Rsph9 was localized to a subpopulation of cilia, whereas they were non-motile. Live imaging of mouse choroid plexus revealed that neonatal CPEC cilia could beat vigorously, and the motility waned and was lost within 1–2 weeks. The beating characteristics of neonatal CPEC cilia were variable and different from those of typical 9+2 cilia of ependyma, yet an Efhc1-mediated mechanism to regulate the beating frequency was shared in both types of cilia. Notably, ultrastructural analysis revealed the presence of not only 9+0 but also 9+2 and atypical ciliary subtypes in neonatal CPEC. Overall, these results identified both conserved and variable components of sensory cilia, and demonstrated a novel mode of ciliary development in mammals.

Key words: Proteomics, Cilia, Development

Introduction

Cilia are projections from the cell surface bearing microtubule-based cytoskeleton, and are involved in various developmental and physiological events (Gerdes et al., 2009). Being present in most cell types in vertebrate, they are highly diverse in their structure and function (Satir and Christensen, 2007; Takeda and Narita, 2012). Regarding the structural aspects, variations exist in the axonemal structure and the ciliary number among different ciliary subtypes. It is well described that the solitary 9+0 primary cilia and multiple 9+2 cilia are generated by distinct cellular mechanisms from each other. Whereas primary cilia are generated in the G_1/G_0 phase by diverting the centriole to the basal body, 9+2 multiciliogenesis involves the explosive neogenesis of basal bodies around the deuterosome deep inside the cytosol (Beisson and Wright, 2003; Dawe et al., 2007; Guirao et al., 2010; Vladar and Stearns, 2007).

Ciliary functions can be generalized as motile propeller and/or sensory antenna, but they are in fact highly variable. Although studies have uncovered intracellular ciliary transport and targeting mechanisms (Nachury et al., 2010), the whole picture is far from being understood. Proteomic analysis of ciliary proteins could provide versatile information to understand ciliary functions as well as ciliary targeting mechanisms. However, cilia proteome, particularly that of 9+0 cilia, is not easily available, largely due to the technical difficulties in isolation of the minute organelle. Among several proteomic analyses of cilia reported so far, most of the datasets were derived from motile 9+2 cilia and flagella (Broadhead et al., 2006; Mayer et al., 2009; Ostrowski et al., 2002; Pazour et al., 2005), while those from mouse photoreceptor outer segments (Liu et al., 2007) solely represent the 9+0 cilia proteome dataset.

In the present study, we analyze the proteome of multiple 9+0 cilia in choroid plexus epithelial cells (CPECs) (Narita et al., 2010; Takeda and Narita, 2012). Our analysis of CPEC cilia from juvenile swine identifies 868 proteins. Comparison to other reported ciliome datasets revealed that nearly a half of the CPEC cilia proteins are also present in photoreceptor outer segment. The juvenile swine CPEC ciliome also includes various signaling molecules, and molecules for ciliary motility such as Rsph9, though they are non-motile. Subsequent live cell imaging and

ultrastructural analyses lead to the discovery of transient motile properties of perinatal CPEC cilia, which are associated with the appearance of 9+2 and atypical ciliary subtypes. Altogether, these results provide valuable information for more comprehensive understanding of 9+0 ciliome, and demonstrate structural and functional transitions of CPEC cilia, which represent a novel mode of ciliary development in mammals.

Results

Proteomic analysis of multiple 9+0 cilia from choroid plexus epithelial cells

To determine the proteome of CPEC cilia, they were purified from swine choroid plexus tissue. The swine used for this work were approximately 6 months of age, which is a juvenile stage (weaned but sexually immature), and corresponds to approximately 1–2 month old mice. Treatment of fresh choroid plexi with dibucaine hydrochloride resulted in acute shedding of cilia, as a massive amount of cilia could be pelleted from the supernatant immediately after the treatment (Fig. 1A). The detached cilia were then enriched by differential centrifugation and equilibrium sedimentation, with more stringent sucrose gradients than previously described (Narita et al., 2010). The enriched fractions of CPEC cilia proteins (~13 µg) were resolved on 5–20% (w/v) polyacrylamide gradient gels, which were cut into four slices and treated with trypsin. The resulting trypsin digests extracted from each gel slice were separated and identified by nano liquid chromatography-mass spectrometry (LC-MS). By using LTQ Orbitrap Velos, 1,115 proteins were identified by 22,431 unique peptides under highly stringent conditions; the precursor mass tolerance, fragment mass tolerance, and false discovery rate were set to 7 ppm, 0.5 Da, and 1%, respectively. However, the protein identities were provisional in most cases because the annotation of swine proteins used for the identification was not as thorough as those of common organisms such as human or mouse. Therefore, we analyzed the identified swine proteins, first by the HomoloGene and second by the Blastp, and the information on human proteins of the highest similarities, including their GO terms, were added to the swine proteome dataset for approximate analyses (supplementary material Table S1).

In the proteome, alpha and beta tubulins were identified with the top 5% probability scores. The dataset also included some intraflagellar transport components (IFT81, IFT122), basal body/transition zone components (ODF2, CEP290, CEP110), septin and importins (SEPT3, IPO4, IPO5), as well as annexins (ANXAs 1, 2, 4, 7, 11), which have been detected in cilia of various mammalian tissues (Ignotz et al., 2007; Ostrowski et al., 2002; Rodrigo et al., 2004) (supplementary material Table S1).

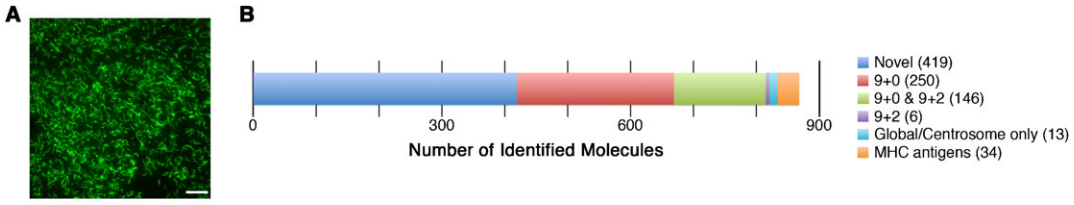

C

Biological Process

GO ID	GO term	Count	P-value	Fold Enrichment
0008104	Protein localization	98	6.99E-14	2.2
0046907	Intracellular transport	77	4.05E-12	2.3
0007010	Cytoskeleton organization	45	6.92E-06	2.1
0016044	Membrane organization	41	7.01E-06	2.2
0032989	Cellular component morphogenesis	42	8.09E-06	2.1

Molecular Function

GO ID	GO term	Count	P-value	Fold Enrichment
0008092	Cytoskeletal protein binding	60	7.52E-10	2.4
0005525	GTP binding	41	3.94E-06	2.2

Cellular Component

GO ID	GO term	Count	P-value	Fold Enrichment
0000267	Cell fraction	131	9.03E-22	2.4
0005783	Endoplasmic reticulum	112	2.43E-17	2.3
0031982	Vesicle	87	4.47E-16	2.6
0012505	Endomembrane system	89	5.43E-13	2.2

Fig. 1. Proteomic analysis of swine choroid plexus epithelial cilia. (**A**) Swine CPEC cilia detached by dibucaine hydrochloride. Crude cilia in suspension were ultracentrifuged, and the resulting pellet was fixed and immunostained for acetylated alpha tubulin (Green). Bar, 20 µm. For proteomic analysis, detached cilia were enriched further by differential centrifugation followed by equilibrium sedimentation. (**B**) Analysis of CPEC cilia proteomics data using the Ciliome database. A database search of molecules identified in the present study was performed. If molecules were already listed, the types of cilia the data were derived from were determined; *9+0*, proteome of mouse photoreceptor sensory cilia (Liu et al., 2007); *9+2*, proteome of motile cilia and flagella from human bronchial epithelium (Ostrowski et al., 2002), Chlamydomonas (Pazour et al., 2005), and trypanosome (Broadhead et al., 2006); *Global*, datasets were obtained by comparative genomics (Avidor-Reiss et al., 2004; Li et al., 2004), transcriptional profiling of Chlamydomonas (Stolc et al., 2005), and analysis of genes containing an x-box in *C. elegans* (Blacque et al., 2005; Efimenko et al., 2005); *Centrosome*, proteome of centrosome from human lymphoblastoma (Andersen et al., 2003) and Chlamydomonas (Keller et al., 2005). The actual counts of molecules in each category are shown in the key. (**C**) Gene ontology terms enriched in the CPEC ciliome. The dataset of 868 CPEC ciliome was analyzed using the DAVID server. Shown in this panel are those with more than 40 gene counts, $P<0.01$, and more than 2-fold enrichment values.

These data indicated that cilia were enriched successfully. However, analysis of the dataset using a mitochondrial proteome database suggested that 15% of identified proteins (185 proteins) might be derived from mitochondria, which have similar physical properties of size and density to cilia and could not be separated completely (supplementary material Table S1). We also checked obvious contaminants such as ribosomal proteins and serum proteins manually (Liu et al., 2007), which altogether added up to an additional 5.6% of total proteins (62 proteins) (supplementary material Table S1). Therefore, we considered the remaining 868 proteins to be the "true" CPEC ciliome.

We next analyzed the CPEC ciliome using the Ciliaproteome database to compare the similarities and differences between previously reported cilia proteomes (Fig. 1B; supplementary material Table S1). This result indicated that approximately half (415 out of 868 proteins) of the CPEC ciliome were shared with other ciliome datasets. Most of the shared proteins (396 proteins) were found in the dataset for the mouse photoreceptor sensory (9+0) cilium complex (Liu et al., 2007). Among the 396 proteins, 250 were those found only in the photoreceptor sensory cilium complex and the remaining 146 were those found in both 9+0 and 9+2 cilia proteome datasets. A small fraction of the CPEC ciliome was shared exclusively with 9+2 cilia and flagella proteome datasets (6 proteins) or other omics datasets (13 proteins) (Fig. 1B). The remaining proteins (34 MHC antigens and 419 other proteins) were not shared with other ciliome datasets (Fig. 1B), suggesting functional diversities among different cilia.

We also performed an approximate GO analysis of the swine CPEC ciliome. Among the total 1,115 proteins identified by LC-MS, 1,068 proteins (96%) were assigned homologous human proteins and 1,060 proteins (95%) were annotated with at least one GO term. The GO terms were then analyzed by using the functional annotation clustering tools of DAVID application server (Huang et al., 2008) (Fig. 1C). In the GO domain of "biological process", enriched GO terms with more than 40 gene counts were "protein localization", "intracellular transport", "cytoskeleton organization", "membrane organization" and "cellular component morphogenesis". In the GO domain of "molecular function", enriched GO terms were "cytoskeletal protein binding" and "GTP binding". In the GO domain of "cellular component", enriched GO terms were "cell fraction", "endoplasmic reticulum", "vesicle" and "endomembrane system". Overall, these data suggested that the molecules involved in ciliogenesis and ciliary transport were enriched in this CPEC ciliome dataset.

Furthermore, to gain insight into the functions of CPEC cilia, enriched GO terms in the subsets of CPEC ciliome were analyzed by DAVID application server. In the 419 CPEC-specific ciliome dataset (*Novel* subset, Fig. 1B), components of various extracellular signaling pathways and small molecule transporters were enriched (Table 1). In the dataset of 250 proteins found only in 9+0 cilia (*9+0* subset, Fig. 1B), enriched GO terms included "vesicle-mediated transport" ($P=4.68\times10^{-5}$), "cofactor binding" ($P=2.37\times10^{-4}$), "enzyme binding" ($P=4.87\times10^{-4}$), "oxidation reduction" ($P=5.45\times10^{-4}$), and "regulation of cellular protein metabolic process" ($P=7.18\times10^{-4}$). Of particular interest was "vesicle-mediated transport", in which several molecules known to localize to cilia or be involved in cilia-mediated processes, such as FLNA (Adams et al., 2012), GSN (Kim et al., 2010), and TXNDC5 (Liu et al., 2007), were found. Collectively, these data demonstrated that a notable molecular similarity between CPEC cilia and photoreceptor outer segment, and provided insight into the common and variable functional aspects of 9+0 cilia.

Identification of motile cilium components in the CPEC ciliome

Interestingly, we identified several molecules in the CPEC ciliome that have been implicated in the motility of 9+2 cilia,

Table 1. Gene ontology terms enriched in the CPEC-specific ciliome. The datasets of the 419 CPEC-specific ciliome and the 868 whole CPEC ciliome were analyzed using the DAVID server. The results were compared to each other, and those GO terms showing higher enrichment scores and greater significance in the CPEC-specific dataset were extracted. Shown below are those with more than 6 gene counts, $P<0.01$, and more than 2-fold enrichment values.

Biological process				
GO ID	GO term	Count	P-value	Fold enrichment
0032868	Response to insulin stimulus	10	6.97E–04	4.1
0051056	Regulation of small GTPase mediated signal transduction	16	1.23E–03	2.6
0007219	Notch signaling pathway	7	1.52E–03	5.6
0015837	Amine transport	10	2.25E–03	3.5
0009991	Response to extracellular stimulus	14	2.72E–03	2.6
0007243	Protein kinase cascade	19	3.93E–03	2.1
0007167	Enzyme linked receptor protein signaling pathway	18	4.04E–03	2.2
0018108	Peptidyl-tyrosine phosphorylation	6	4.87E–03	5.4
0006820	Anion transport	10	7.95E–03	2.9
0051272	Positive regulation of cell motion	8	9.58E–03	3.4
Molecular function				
GO ID	GO term	Count	P-value	Fold enrichment
0004672	Protein kinase activity	31	2.74E–04	2.0
0005158	Insulin receptor binding	6	5.75E–04	8.6
0005178	Integrin binding	7	3.42E–03	4.7
Cellular component				
GO ID	GO term	Count	P-value	Fold enrichment
0043235	Receptor complex	11	3.48E–04	4.1

namely, deleted in primary ciliary dyskinesia (Zariwala et al., 2004) and radial spoke head homologs 4a and 9 (Castleman et al., 2009) (supplementary material Table S1). To validate the proteome data, the mRNA levels of the aforementioned motile cilium components in mouse CPECs were compared by the comparative C_T method to those in ependyma (expressing motile 9+2 cilia and therefore served as a positive control) and in serum-starved NIH3T3 cells (expressing non-motile 9+0 primary cilium and therefore served as a negative control). The quality of primary cultures was validated based on the presence of characteristic cilia (Fig. 2A), as well as real-time PCR for well-known molecular markers of ependymal cells (CD24a) and CPECs (transthyretin; TTR) (Fig. 2B). The motility of ependymal cilia was also confirmed by light microscopy. The expression of Foxj1, the master regulator of motile cilia specification known to be expressed in choroid plexus (Lim et al., 1997), was also confirmed in CPECs, although the levels were somewhat lower than those in ependymal cultures (Fig. 2B). These data demonstrated that the mRNAs of motile cilium components were expressed in CPECs, and that the levels were either comparative to ependyma or intermediate between ependyma and NIH3T3 cells.

Next, we focused on one of the motile cilium components, Rsph9, and assessed its ciliary localization in CPECs. The specificity of the antibody was validated by western blotting for Rsph9 using whole cell lysates of mouse sperm, ependymal cells and HEK293 cells transiently overexpressing Rsph9-FLAG (Fig. 3A; data not shown). Consistent with real-time PCR data, Rsph9 protein was also detected in mouse CPECs by western blotting, but levels were as low as 3% of those in ependymal cells (Fig. 3B). In adult mouse brain sections, both the ependymal cilia and some choroid plexus epithelial cilia were immunostained for Rsph9 (Fig. 3C). In the ependymal layer, the cytoplasm was also stained to some extent, which may be a reservoir of Rsph9 and suggest its rapid turnover in this cell type. Ciliary localization of Rsph9 protein was also observed in juvenile swine choroid plexus tissue (Fig. 3D, top panel); the swine CPEC cilia were longer than mouse counterparts and therefore easier to observe. Interestingly, both mouse and swine CPEC cilia always showed some heterogeneity with respect to Rsph9 immunoreactivity, even in single cells (Fig. 3D, top panel; data not shown). In purified swine CPEC cilia, Rsph9-positive cilia accounted for ~40% of the total population (Fig. 3D, bottom panel; Fig. 3E). These results demonstrated that Rsph9 protein was expressed and localized in a subset of CPEC cilia in juvenile swine and adult mouse, consolidating the proteome data.

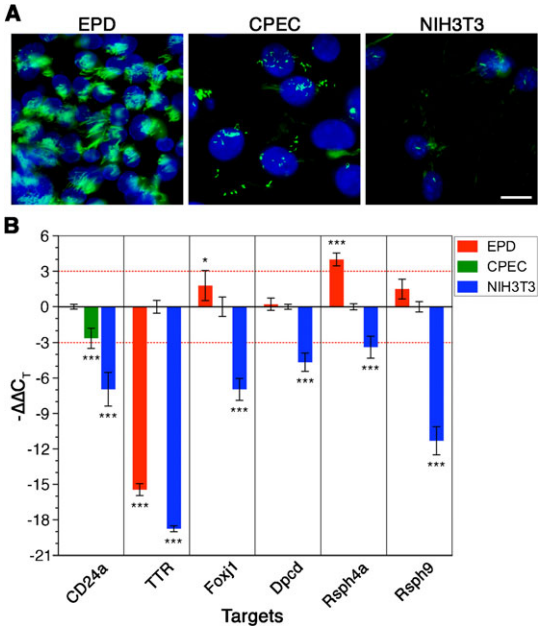

Fig. 2. Validation of motile cilium component gene expression in choroid plexus epithelium. (**A**) Primary cultures of mouse ependyma (EPD; left), choroid plexus epithelium (CPEC, middle) and serum-starved NIH3T3 cells (right). Cells were immunostained for acetylated alpha tubulin (Green). Cell nuclei were counter-stained with DAPI (Blue). Bar, 16 µm. (**B**) Real-time PCR analysis. The gene expression levels of motile cilium components (Dpcd, Rsph4a and Rsph9) identified by the CPEC ciliome were assessed by the comparative C_T method. RNA samples from EPD and CPEC were prepared from mouse primary cultures, and their qualities were validated by the expression levels of CD24a (EPD marker) and transthyretin (TTR; CPEC marker). The $-\Delta\Delta C_T$ values were calculated using B2m as an endogenous reference and CPEC as a calibrator. For CD24a, EPD was used as a calibrator. Values were expressed as the mean ± s.d. *, $P<0.5$; **, $P<0.01$; ***, $P<0.001$ versus calibrator.

CPEC cilia are motile at birth and become non-motile during aging

Previously, we observed CPEC ciliary motility using swine primary cultures in a preliminary setup and found that they were non-motile under normal culture conditions (Narita et al., 2010). However, this observation was contradictory to an earlier report briefly describing a very slow beating of choroid plexus cilia in rodents (Roth et al., 1985). This report was based on a measurement of oscillatory changes in the light intensity transmitted through moving cilia in the brain ventricles detected by a fine optic fiber, and provided no information on detailed beating characteristics, such as beating form and orientation. Having identified the motile cilium components in the ciliome, as well as to resolve the apparent contradiction, we examined CPEC ciliary motility again. Live microscopy of swine CPEC primary cultures, as well as swine choroid plexus tissue all indicated that most, if not all, CPEC cilia were standing still, consistent with our previous observation (supplementary material Movie 1). We also drew the same conclusion from the examination of juvenile (P28) and adult mouse choroid plexus tissue (Table 2). These data indicated that the Rsph9 in swine and mouse CPEC cilia at juvenile and adult stages were non-functional or vestigial, from the viewpoint of ciliary motility.

We next sought to examine the CPEC ciliary motility in younger animals. For this analysis, we focused on mouse, due to the difficulty in obtaining varying ages of swine as well as to the good phenotypic matches between swine and mouse samples as described above. When newborn choroid plexus tissue was examined, active beating of many, but not all, CPEC cilia was found (supplementary material Movie 1). Interestingly, the motility of CPEC cilia waned as mice grew, and approximately two weeks after birth, finding motile CPEC cilia became difficult and the beating appeared to be feeble (supplementary material Movie 1). These data demonstrated that newborn CPEC cilia were able to beat, and within 1–2 weeks, lost motility and eventually became non-motile (Table 2).

The beating characteristics of neonatal mouse choroid plexus cilia

We analyzed the ciliary motilities of mouse CPECs and ependymal cells in more detail using high-speed video

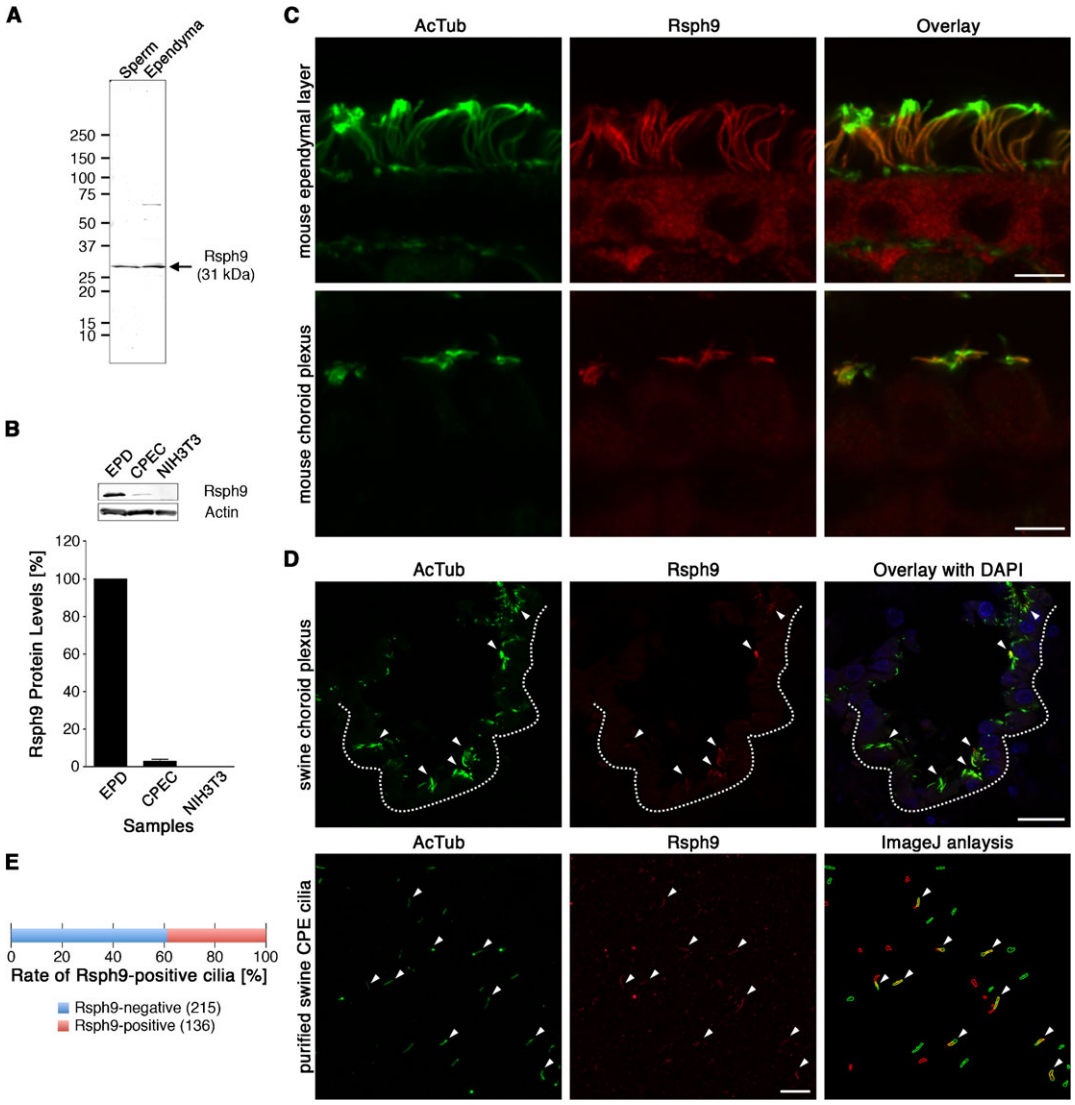

Fig. 3. Immunological analysis of Rsph9. (**A**) Western blot analysis for Rsph9. Whole cell lysates from mouse sperm and ependymal cell cultures (10 µg of total protein each) were used for the analysis, yielding an immunoreactive band of ~31 kDa. The positions and sizes (kDa) of the molecular weight standard are indicated on the left. (**B**) Top, comparison of Rsph9 protein levels between ependyma (EPD), choroid plexus epithelium (CPEC), and NIH3T3 cells. The immunoblot for actin shows equal loading. Bottom, quantification of Rsph9 protein levels by image analysis (n=4). (**C**) Immunostaining of adult mouse brain sections for acetylated alpha tubulin (Green) and Rsph9 (Red). The panels shown are the ependymal layer (top) and choroid plexus (bottom). Bars, 5 µm. (**D**) Immunostaining of swine choroid plexus tissue (top) and purified swine choroid plexus cilia (bottom) for acetylated alpha tubulin (Green) and Rsph9 (Red). For the top panel, cell nuclei were counter-stained with DAPI (Blue). Arrowheads indicate Rsph9-positive cilia. Note the uneven distribution of Rsph9, suggesting the heterogeneity of CPEC primary cilia in terms of motility. Bars, 20 µm. (**E**) Quantification of Rsph9-positive cilia by image analysis of purified swine choroid plexus cilia shown in D.

microscopy and compared the beating characteristics. Contrary to our expectation that CPEC cilia have 9+0 axoneme and should therefore rotate rather than beat as in the case of nodal cilia (Takeda et al., 1999), most of the motile CPEC cilia showed a planar back-and-forth motion, whereas a few of them exhibited rotational movements (Fig. 4A; supplementary material Movie 2). The characteristics of CPEC ciliary movement were nevertheless distinct from those of ependymal cilia. First, while cultured ependyma exhibited uniform ciliary beating forms (Fig. 4A; supplementary material Movie 2), those of neonatal CPECs were variable. Based on the motility characteristics, CPEC cilia appeared to be classified into four subgroups (Fig. 4B): (1) fast beat (average-high ciliary beat frequency (CBF)); (2) slow beat (low CBF); (3) rotation; (4) non-motile. The beating amplitude of CPEC cilia (2.0±0.7 µm, n=20 from 3 cells) was also smaller than that of ependymal cells (7.0±1.9 µm, n=11 from 2 cells) (Fig. 4A,B). Second, the CBF was lower in neonatal CPEC (8.1±2.5 Hz; excluding non-motile cilia) in comparison with ependymal cells (19.1±4.5 Hz) (Fig. 4C,D). Moreover, ependymal CBF followed normal

Table 2. Changes in ciliary motility scores in mouse CPECs following postnatal development.

Postnatal days	Ciliary motility scores
P1	++
P7	+
P14	+/−
P28-adult	−

++: high, +: moderate, +/−: low, −: absent

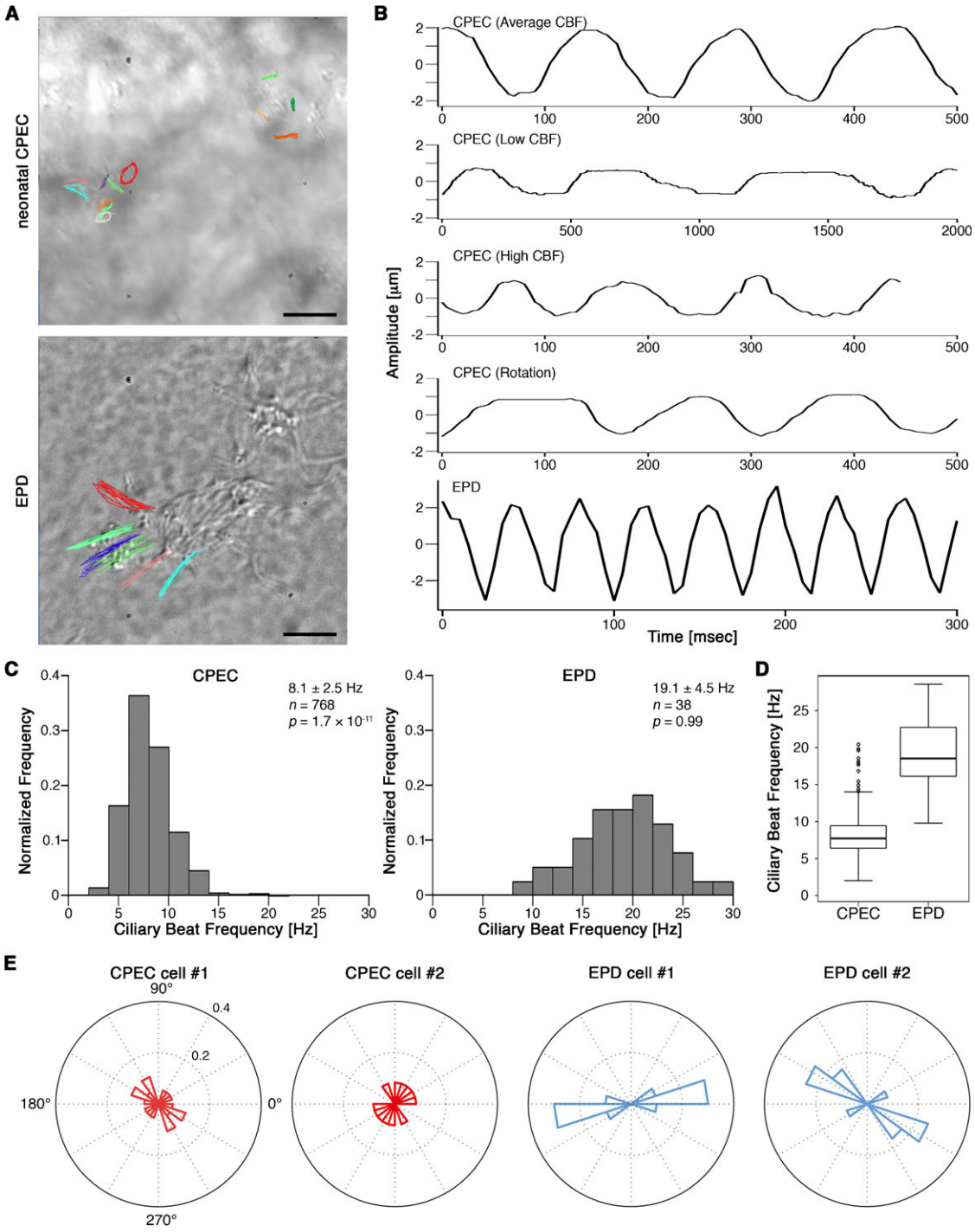

Fig. 4. Characterization of newborn CPEC ciliary motility. (**A**) Top view snapshots of neonatal mouse CPEC (top) and differentiated ependymal cultures (bottom) observed by high-speed video microscopy. The tips of individual cilia were traced manually. Note the presence of both beating and rotating cilia, small beating amplitude and random beating orientation in CPECs. The original live imaging data are available in supplementary material Movie 2. Bars, 5 µm. (**B**) Representative plots of CPECs and ependymal ciliary tip movements. For each ciliary tip tracing, the long axis was determined and defined as the Y-axis of the plot. (**C**,**D**) Summary histograms (C) and box-and-whisker plots (D) of ciliary beating frequency showing differences between neonatal CPECs and differentiated ependymal cultures. (**E**) Circular histograms showing the angular distribution of ciliary beating axes in single cells. The data were normalized to the number of tracked cilia, and each element of the histogram was drawn in point symmetry to the center of the graph.

distribution (P=0.99, chi-square test), while CPECs did not (P=1.7×10^{-11}), likely reflecting the aforementioned heterogeneity. Third, unlike mature ependymal cilia that all beat in the same direction at the cellular and tissue level (Guirao et al., 2010), the beating of neonatal CPEC cilia appeared to be in random orientations (Fig. 4E).

To gain insight into the molecular basis of CPEC ciliary motility, we analyzed the neonatal CPEC cilia from *Efhc1*

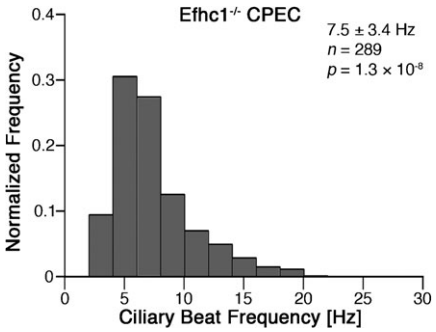

Fig. 5. Measurement of newborn Efhc1$^{-/-}$ CPEC ciliary beating frequency. A summary histogram of ciliary beating frequency in CPECs from neonatal Efhc1 knockout mice, showing significantly lower beating frequency than wild-type ($P=1.3\times10^{-8}$, Mann-Whitney test).

knockout mice. Efhc1 is a microtubule-associated protein localized to mature ependymal cilia and regulates their beating frequency (Suzuki et al., 2009). Interestingly, Efhc1 is expressed transiently in the fetal choroid plexus (Suzuki et al., 2008), which appeared to correlate with the change of ciliary motility in these cells after perinatal period. High-speed video microscopy indicated that the CBF of CPEC from *Efhc1* null mice (7.5±3.4 Hz) was significantly lower than that of wild type (8.1±2.5 Hz; $P=1.3\times10^{-8}$, Mann-Whitney test) (Fig. 4C, Fig. 5), which was similar to the previous report demonstrating the effect of *Efhc1* knockout on CBF of mature ependymal cilia (Suzuki et al., 2009). Collectively, these data demonstrated that, although the characteristics of ciliary motility in CPEC and ependyma were distinct from each other, they share a common, Efhc1-mediated molecular mechanism to regulate the motility.

The axonemal structure of neonatal mouse choroid plexus epithelial cilia was a mixture of 9+0, 9+2 and atypical variants

We and others have previously demonstrated that juvenile and adult CPECs possess clusters of 9+0 cilia (Madhavi and Jacob, 1989; Peters et al., 1991; Narita et al., 2010). However, the observed planar beating strongly suggested that they were 9+2 cilia; indeed, the central pair is believed to define the beating form, as well as the beating plane (Hirokawa et al., 2009; Yagi and Kamiya, 2000). Therefore, we investigated the axonemal structure of neonatal CPEC cilia. For this, the choroid plexus epithelial cilia of the lateral ventricles from P1 mouse pups were fixed and investigated by transmission electron microscopy (TEM) (Fig. 6A,B). Surprisingly, but consistent with the motility profile, ciliary axonemal structure of neonatal CPECs were found out to be heterogeneous. While the majority of cilia possessed the 9+0 axoneme and its variants (Fig. 6B,C), the others clearly had an electron-dense, microtubule-like structure at the center, surrounded by nine outer doublets. Detailed ultrastructural inspection revealed that they took not only the 9+2 but also atypical 9+1 configurations, in which one central doublet microtubule was surrounded by nine outer doublets (Fig. 6C). Of note was the hybrid nature of CPEC cilia; namely, 9+0, 9+2 and

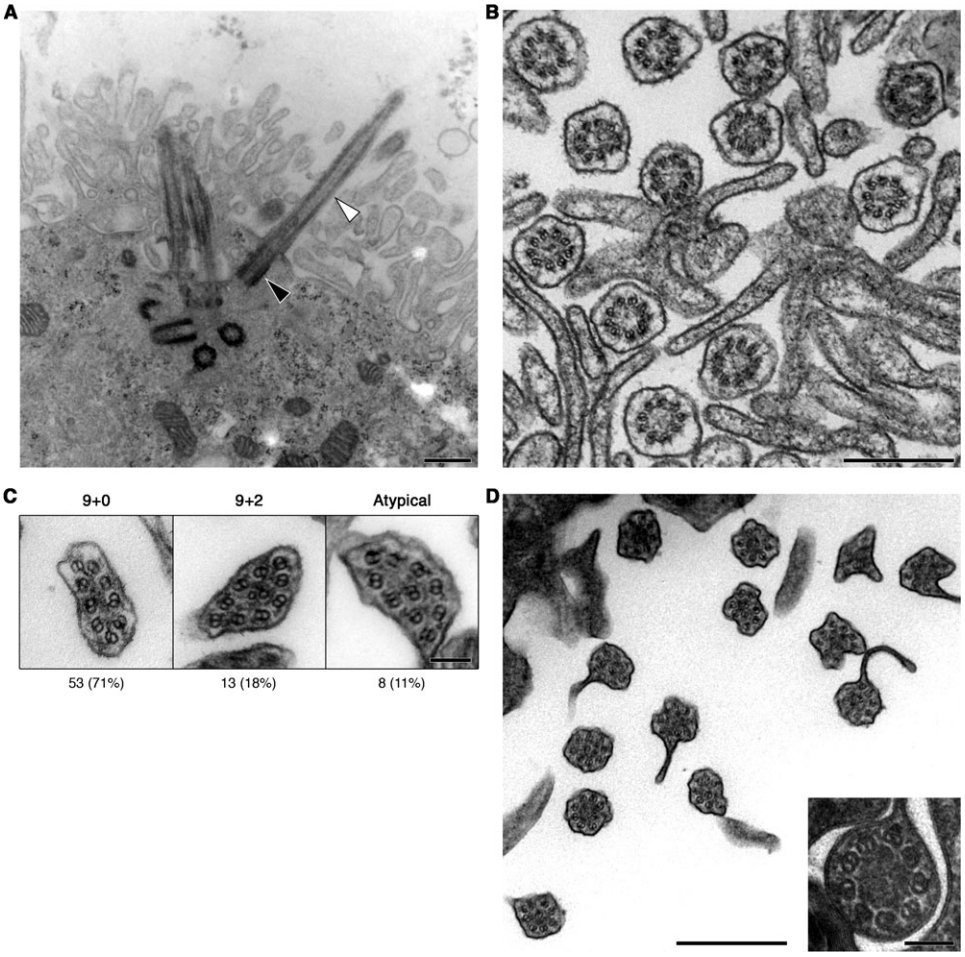

Fig. 6. Ultrastructural analysis of neonatal mouse CPEC cilia. Representative longitudinal (**A**) and transverse (**B**) sections of neonatal mouse CPEC cilia. In (A), the basal body and ciliary axoneme were highlighted with black and white arrowheads, respectively. The ciliary axonemes shown in (B) all took 9+0 configuration. Bars, 500 nm.
(**C**) Summary of the ultrastructural analysis of neonatal mouse CPEC cilia. The axonemal structures of 74 cilia were investigated and classified into three categories. Bar, 100 nm.
(**D**) A representative transverse section of juvenile swine CPEC cilia, which all took 9+0 and the derived configurations. Due to an unavoidable delay in fixing the swine tissue at slaughterhouse, the membrane structure was damaged. Bar, 500 nm. Inlay, magnified view. Bar, 100 nm.

atypical 9+1 variants were found on the same cell (supplementary material Fig. S1). We also noted that neonatal CPEC cilia were flattened in many cases. By contrast, in juvenile swine CPECs in tissue, we observed only 9+0 cilia and its variants (Fig. 6D), consistent with our previous data using juvenile swine CPEC primary culture (Narita et al., 2010). These data suggested that the transient ciliary motility in perinatal CPEC were coincident with the generation of 9+2 and atypical 9+1 cilia.

Discussion

To gain insight into the functional and developmental diversities of cilia, the proteome of multiple 9+0 cilia from juvenile swine CPECs were analyzed. Largely due to the incomplete swine protein annotation, full identification of known cilia proteins, such as IFT proteins and Kif3A/B, was not achieved. There were in fact many MS spectra that were left unidentified. Future enrichment of swine protein database will resolve this issue. Nevertheless, we identified 868 proteins including many membrane channels and receptors as CPEC ciliome, which is comparative to the number of proteins in photoreceptor outer segment (1,185 proteins) (Liu et al., 2007). As proposed by the authors, the large number of proteins in CPEC cilia may reflects the complexities in the ciliary function and the swine genome. Notably, though the photoreceptor outer segment and CPEC cilia are specialized and multiple 9+0 cilia, respectively, nearly 50% of protein components are conserved (Fig. 1).

During preparation of this manuscript, proteome of "generic" primary cilia from mouse inner medullary collecting duct 3 (IMCD3) cells was reported by Ishikawa and colleagues, identifying shared and variable components among different cilia proteome datasets (Ishikawa et al., 2012). Our CPEC cilia proteome dataset in combination with other ciliome datasets provides comprehensive information on what proteins are actually transported to cilia, and will therefore contribute to a better understanding of ciliary targeting mechanisms as well as the functional diversity.

The present study goes beyond the proteomic analysis by providing an insight into the development of CPEC cilia. While the cellular events associated with ciliogenesis of solitary 9+0 primary cilia and multiple 9+2 cilia are well described, that of multiple 9+0 cilia in CPECs was totally unknown. Our analysis of the CPEC cilia proteome also led to the discovery that CPEC ciliary motility is lost progressively after birth (Table 2). This is in clear contrast to the typical multiciliogenesis in bronchial epithelium or the ependyma, wherein fetal 9+0 cilia are replaced by 9+2 cilia, leading to full-fledged motile cilia (Sorokin, 1968; Spassky et al., 2005; Vladar and Stearns, 2007). Subsequent analyses of ciliary beating characterization and axonemal structure strongly suggested that CPEC cilia are derived originally as motile cilia that take 9+2 or atypical 9+1 axonemal configurations, and then shifted to non-motile 9+0 cilia (Figs 4–6), representing a novel mode of ciliary development in mammals.

Interestingly, Mair and colleagues reported that frog olfactory epithelium bore different types of cilia; one was short, motile and newly generating cilia, whereas the other was long, immotile and mature cilia (Mair et al., 1982). These observations appear to be reminiscent of the developmental changes in CPEC ciliary motility described in the present study. In this sense, the loss of motility in CPEC cilia may correlate with the degree of ciliary and/or cellular maturations, and a similar mode of ciliary development might be facilitated in other cell type to generate multiple, specialized cilia. These reports and our findings may pave the way into the evolutionary changes of ciliary types in light of the phylogeny of cilia.

We initially expected that the perinatal CPEC ciliary beating might contribute to the circulation of CSF, because most ependyma have unestablished motile cilia by this time, and it would take approximately three weeks after birth for full maturation (Spassky et al., 2005). However, detailed analyses of neonatal CPEC ciliary motility demonstrated that beating was of low frequency as described previously (Roth et al., 1985), of small amplitude and random orientation (Fig. 4). Since Tissir et al. also reported that mutations in the planar cell polarity genes, *Celsr2* and *Celsr3*, impaired ciliogenesis in ependymal cells while CPEC ciliogenesis was unaffected (Tissir et al., 2010), it is likely that the ciliary motility of perinatal CPECs have different functions from that of the ependyma. Although the transient ciliary motility might simply happen without functional significance during this mode of multiciliogenesis, one of our current speculations is that CPEC ciliary beating may be assisting radial diffusion of molecules that are secreted from CPECs into the CSF. Such assistance may be crucial, for example, in volume transmission of CPEC-derived signaling molecules that would affect the development of cells around brain ventricles (Guirao et al., 2010).

Our gene ontology analysis demonstrated that various signaling molecules were enriched in the CPEC-specific ciliome components (Table 1). This result was consistent with the fact that CPECs express a wide array of cell signaling receptors and ligands (Chodobski and Szmydynger-Chodobska, 2001; Narita et al., 2010), and have multiple functions to maintain brain homeostasis, such as the production of CSF (Narita et al., 2010), receptor-mediated material transport across the blood-CSF barrier (Mitchell et al., 2009), and recruit of lymphocytes for immunosurveillance of the central nervous system (Reboldi et al., 2009). Our data support the idea that mature, non-motile CPEC cilia may be involved in such multiple, tissue-specific signaling events. The present study will be a toehold for getting a deep insight in the brain function through a showcase of ventricular system, and for better understanding of the functional and developmental diversities of vertebrate cilia.

Materials and Methods

Isolation of swine choroid plexus cilia

Isolation of swine CPEC cilia was performed as described previously (Narita et al., 2010) with modifications. In brief, fresh choroid plexus tissue, dissected from swine brains at the local slaughterhouse (Yamanashi Meat Logistics Center, Yamanashi, Japan), was treated with 1 mM dibucaine hydrochloride (Wako Pure Chemical Industries, Osaka, Japan) in ice-cold Dulbecco's modified Eagle medium (DMEM)/HAM's F12 (1:1) (Invitrogen Japan, Tokyo, Japan) containing 0.25 M sucrose for 1 min with gentle agitation at 4℃. After centrifugation at 1,000 × g for 10 min at 4℃, the detached cilia in the resulting supernatant were sedimented on a 50% (w/v) sucrose cushion at 6,000 × g for 10 min at 4℃. The enriched materials on the cushion were collected, overlaid on 9 ml of a 42.5%/40% (w/v) discontinuous sucrose gradient in a 13-ml ultracentrifuge tube, and subjected to equilibrium sedimentation at 150,000 × g for 2 h at 4℃. The cilia enriched at the interface were collected by punching a hole on the side of the tube using a syringe fitted with a 23-G needle, pelleted at 20,000 × g for 5 min at 4℃, and stored at −80℃ until ready for use. The presence of intact cilia in the final pellet was validated routinely by immunostaining for acetylated alpha tubulin. Total protein concentration was determined using Protein Assay Bicinchoninate Kit (Nakalai Tesque, Kyoto, Japan).

Protein identification by mass spectrometry and data analysis

For proteomic analysis, 13 μg of total protein in the isolated CPEC cilia fraction was dissolved in 4× SDS sample buffer and electrophoresed on a precast 5–20% (w/v) e-PAGEL (ATTO. Tokyo, Japan). The gel area containing 20–250 kDa

proteins was cut into four slices using a clean razor blade, and each slice was transferred into a new tube. After reduction and alkylation, the samples in the gel were digested with trypsin overnight at 37℃. The resulting digests were extracted from the gel, concentrated to ~20 µl, and separated on a reversed-phase column using a DiNa-2A nano-LC system (KYA Technologies, Tokyo, Japan). The mobile phases consisted of solvent A (2% (v/v) acetonitrile and 0.1% (v/v) formic acid in H_2O) and solvent B (80% (v/v) acetonitrile and 0.1% (v/v) formic acid in H_2O). The peptides were eluted from the column with a three-step linear gradient of solvent B: 0 to 15% in 20 min, 15 to 50% in 105 min and 50 to 100% in 5 min at a flow rate of 300 nl/min, and sprayed into a LTQ-Orbitrap Velos (Thermo Fisher Scientific, Waltham, MA, USA), which was operated in data-dependent mode, automatically switching between MS and MS/MS acquisition. Full-scan MS spectra (from m/z 380 to 2,000) were acquired in the orbitrap with a resolution of 100,000 at m/z 400. The 20 most intense ions at a threshold above 1,000 were fragmented for collision-induced dissociation in the linear ion trap with normalized collision energy of 35%. All MS spectra were recalibrated in real time with the lock mass option (Olsen et al., 2005) to improve the mass accuracy.

The acquired MS/MS spectra were searched against a non-redundant protein database (Other mammalia; May 15, 2010) from the National Center for Biotechnology Information (NCBI) using the Mascot (v.2.2.04) algorithm (Matrix Science, Boston, MA, USA) with the following parameters: fixed modifications, carbamidomethylation of cysteines; variable modifications, methionine oxidation, pyro-glutamination for *N*-terminal glutamine, *N*-terminal acetylation; maximum missed cleavages, 2; peptide mass tolerance, 7 ppm; MS/MS tolerance, 0.5 Da; false discovery rate, 1%. Finally, 1,115 Sus scrofa proteins were extracted by 5,525 unique peptides.

Because swine protein annotation was not as thorough as those of humans, each protein in the dataset was first assigned a homologous human protein using the HomoloGene database (http://www.ncbi.nlm.nih.gov/homologene) and Blastp (http://blast.ncbi.nlm.nih.gov) for approximate analyses. When multiple swine protein entries yielded the same human protein, the redundancy was maintained. To check if the proteins were derived from contaminants such as mitochondria, serum, or ribosomes, the dataset was analyzed using the MitoProtein database (http://www.mitoproteome.org) and manual investigation. Following these analyses, 247 proteins were marked as probable contaminants, and the remaining 868 proteins were treated as the "true" CPEC ciliome. For comparison of the CPEC cilia proteome with other ciliome datasets, the dataset was analyzed using the Ciliaproteome database (http://www.ciliaproteome.org). For gene ontology (GO) analysis, the GO terms assigned to human homologs were analyzed using the Entrez Gene database (ftp://ftp.ncbi.nlm.nih.gov/gene/DATA/gene2go.gz; as of September 7, 2010). The GO terms enriched in the CPEC ciliome were identified using the functional annotation clustering tools of DAVID application server (version 6.7; http://david.abcc.ncifcrf.gov/summary.jsp).

Comparison of gene expression levels among choroid plexus epithelium, ependyma and NIH3T3 fibroblasts

Full details of the mouse study were approved by the Institutional Animal Care and Use Committee at the University of Yamanashi (Approval number: 19-92). All mice were handled according to the Guide for the Care and Use of Laboratory Animals. Primary cultures of mouse choroid plexus epithelial cells were prepared as described for swine CPECs (Narita et al., 2010), except that dissociation was performed with 0.38 mg/ml papain and tissue was triturated into small pieces by repeated pipetting through 200-µl micropipette tips after enzymatic treatment. Cells were grown for one week to confluency for RNA extraction. For primary cultures of mouse ependyma, the lateral walls of the lateral ventricles containing the subventricular zone were dissected from P1 mice, triturated by repeated pipetting through 1000-µl and 200-µl micropipette tips, and plated in Neurobasal-A medium containing B-27 and ITS supplements (Invitrogen Japan, Tokyo, Japan). Cells were maintained for 3 weeks for monolayer formation and ciliogenesis, and medium was changed twice a week. Cell debris and contaminated neurons were washed out by applying a stream of culture medium from a pipette before changing the medium. Total RNA was extracted from primary cultures as well as serum-starved NIH3T3 cells using the RNeasy Mini kit (Qiagen Japan, Tokyo, Japan). Total RNA from mouse choroid plexus tissues was extracted using Trizol Reagent (Invitrogen Japan, Tokyo, Japan). Reverse transcription and real-time PCR were performed using the First Strand cDNA Synthesis Kit (Fermentas, Glen Burnie, MD, USA) and Power SYBR Green PCR Master Mix (Applied Biosystems Japan, Tokyo, Japan), respectively, following the manufacturers' instructions. The sequences of custom oligonucleotide primer (Invitrogen Japan, Tokyo, Japan) used for real-time PCR are as follows: CD24a Fwd, 5′-TGCTCCTACCCACGCAGATT-3′; CD24a Rev, 5′-CGGGAAACGGTGCAACA-3′; TTR Fwd, 5′-TCCCTTCGACTCTTCCTCCTT-3′; TTR Rev, 5′-GGGCCAGCTTCAGACACAAA-3′; Foxj1 Fwd, 5′-GCCACAACCTGTCCTTGAACA-3′; Foxj1 Rev, 5′-GCCGGGCTCATCCTTCTC-3′; Dpcd Fwd, 5′-GGGATCCGAGCTCATCAAAG-3′; Dpcd Rev, 5′-GGTGTCCTTGCGCATGAAG-3′; Rsph4a Fwd, 5′-TTGAAGGCATCCAAGTGATTGA-3′; Rsph4a Rev, 5′-TGCACGTGATGAACCCAATT-3′; Rsph9 Fwd, 5′-CCTCTTCAAGACCCCTTTTGG-3′; Rsph9 Rev, 5′-GGGCAGGCCTTCAAAGGT-3′; B2m Fwd, 5′-CACTGACCGGCCTGTATGC-3′; B2m Rev 5′-GGTGGCGTGAGTATACTTGAATTTG-3′.

Western blotting and immunocytochemistry

For western blotting, appropriate amounts of protein were separated by electrophoresis on 5–20% (w/v) SDS poly-acrylamide gels and transferred to Immobilon-P membranes (Millipore, Billerica, MA, USA). After blocking with Tris buffered saline with Tween 20 (TBST) containing 5% (w/v) non-fat dry milk for 1 h at room temperature (RT), the blots were incubated with the primary antibodies diluted 1:500 in the blocking buffer and incubated overnight at 4℃. The blots were then washed with TBST and incubated with alkaline phosphatase-conjugated secondary antibody diluted 1:500 in the blocking buffer at RT for 1 h. After washing with TBST, the immuno-reactive bands were visualized using nitro blue tetrazolium chloride (NBT) and 5-Bromo-4-chloro-3-indolyl phosphate, toluidine salt (BCIP) substrates (Roche Diagnostics Japan, Tokyo, Japan). The antibodies used for immunostaining were as follows: Rsph9 (HPA031703, Sigma-Aldrich Japan, Tokyo, Japan); FLAG (018-22381, Wako Pure Chemical Industries, Osaka, Japan); pan actin (MS-1295-P0, Thermo Fisher Scientific Japan, Yokohama, Japan); mouse IgG conjugated with alkaline phosphatase (62-6522, Invitrogen Japan, Tokyo, Japan); rabbit IgG conjugated with alkaline phosphatase (G21079, Invitrogen Japan, Tokyo, Japan).

For immunostaining of the choroid plexus and ependymal layer in brain sections, mice were euthanized by cervical dislocation and the brains were dissected out quickly into cold Leibovitz L-15 medium, cut on a coronal plane to open the anterior horn of the lateral ventricles and immersed immediately in fixative solution (4% (w/v) paraformaldehyde, 100 mM HEPES, pH 7.4, 2.5 mM $CaCl_2$, 1.25 mM $MgCl_2$, 2.9% (w/v) glucose). The coronal brain cryosections of 5 µm thickness were mounted on coated glass slides and autoclaved for heat-induced epitope retrieval. On the other hand, cell cultures grown on glass coverslips were fixed with −20℃ methanol. The sections and monolayers were rinsed with PBS, blocked with 5% (w/v) skim milk in PBS for 30 min, and incubated with the primary antibody overnight at 4℃. After washing with PBS, the samples were incubated with the secondary antibody for 30 min at room temperature, washed with PBS and sealed in mounting solution with 4′,6-diamidino-2-phenylindole (DAPI). The stained cells were investigated under an Olympus BX50 microscope equipped with a Keyence VB-7010 cooled CCD color camera and a VB-7000 digital microscope camera control system (Keyence Japan, Osaka, Japan) or Olympus FluoView 1000 confocal microscope. The primary antibodies used for immunostaining and their dilutions were as follows: acetylated alpha tubulin (1:500; clone 6-11B-1, Sigma-Aldrich Japan, Tokyo, Japan) and Rsph9 (1:200). The secondary antibodies used were Alexa Fluor 488-conjugated goat anti-mouse (1:200) and Alexa Fluor 568-conjugated goat anti-rabbit (1:200) (Invitrogen Japan, Tokyo, Japan). As a negative control, normal immunoglobulins were used as the primary antibody.

Live imaging of choroid plexus epithelial cilia

For the observation of mouse CPEC ciliary motility, wild-type (C57Bl/6J, Charles River Laboratories Japan, Yokohama, Japan) and *Efhc1* knockout (Suzuki et al., 2009) mice were used. Animals were euthanized by decapitation and the choroid plexus tissues were dissected out of the brain immediately in cold Leibovitz L-15 medium and transferred to 35-mm glass bottom dishes. Ciliary motility was first investigated using an Olympus ZDC-IMAGE system equipped with differential interference contrast optics, a UPlanSApo 60×/1.35 oil-immersion objective and a Photometrics Coolsnap HQ2 cooled CCD camera. The images were recorded at approximately 11 frames per second with MetaMorph software. For high-speed video microscopy, the tissues were observed with an Olympus IX71 inverted microscope equipped with a 100 W mercury lamp as a light source, differential interference contrast optics, a UPlanSApo 40×/1.15 water-immersion objective, and an Allied GE680 CCD camera, and the images were recorded with typically 1–2 msec exposure time at 200 frames per second and analyzed with TI Workbench software written by Dr. Takafumi Inoue (Fukatsu et al., 2004). Samples were analyzed at room temperature typically within 25–60 min after euthanasia. Primary cultures of mouse ependyma were also observed under video microscopy for comparison. The CBF was calculated using the following formula (Chilvers and O'Callaghan, 2000): [CBF=(number of frames per second)/(average number of frames for single beat)]. To measure the uniformity of the directions of ciliary beating in single cells, tracks of ciliary tips traced from time-lapse images were fitted to eclipses and the angles of long axes were calculated. In each cell, histograms of the angles were calculated, normalized to the number of tracked cilia, and displayed as circular histograms, in which each element of the histogram was drawn in point symmetry to the center of the graph.

Transmission electron microscopy

For TEM of neonatal CPEC cilia, P1 mouse pups were fixed by perfusion with 2% (w/v) paraformaldehyde, 2.5% (w/v) glutaraldehyde and 2% (w/v) tannic acid in 0.1 M cacodylate buffer, pH 7.4. Whole brains were dissected out and fixed in the same fixative overnight at 4℃. In some experiments, fresh P1 choroid plexus

tissue was dissected out and fixed by immersion. The remainder of the procedure was performed as previously described (Narita et al., 2010).

Statistical analysis

All values were expressed as the mean ± s.d. Real-time PCR data were analyzed with two-way ANOVA followed by Bonferroni posttest to compare selected pairs. For ciliary beat frequency data, the chi-square test was applied to test for normal distribution, and Mann-Whitney test to assess differences between wild-type and Efhc1 knockout mice. Results were considered significant at $P<0.05$.

Acknowledgements

We would like to thank Hideaki Hayashi, Hiroaki Tagawa and the staff of Yamanashi Meat Logistics Center and Yamanashi Meat Hygiene Inspection Office for helping with the isolation of the swine choroid plexus tissue. We also thank Kazuko Sawanobori for secretarial assistance and animal work. This research was supported by the Grant-in-Aid for Scientific Research (C) from MEXT (19590188), the Uehara Memorial Foundation, Astellas Foundation for Research on Metabolic Disorders and Yamada Science Foundation to S. T., and the Grant-in-Aid for Young Scientists (B) from MEXT (22770190) to K. N. The funders had no role in study design, data collection and analysis, decision to publish, or preparation of the manuscript.

Competing Interests

The authors declare that there are no competing interests.

References

Adams, M., Simms, R. J., Abdelhamed, Z., Dawe, H. R., Szymanska, K., Logan, C. V., Wheway, G., Pitt, E., Gull, K., Knowles, M. A. et al. (2012). A meckelin-filamin A interaction mediates ciliogenesis. *Hum. Mol. Genet.* **21**, 1272-1286.

Andersen, J. S., Wilkinson, C. J., Mayor, T., Mortensen, P., Nigg, E. A. and Mann, M. (2003). Proteomic characterization of the human centrosome by protein correlation profiling. *Nature* **426**, 570-574.

Avidor-Reiss, T., Maer, A. M., Koundakjian, E., Polyanovsky, A., Keil, T., Subramaniam, S. and Zuker, C. S. (2004). Decoding cilia function: defining specialized genes required for compartmentalized cilia biogenesis. *Cell* **117**, 527-539.

Beisson, J. and Wright, M. (2003). Basal body/centriole assembly and continuity. *Curr. Opin. Cell Biol.* **15**, 96-104.

Blacque, O. E., Perens, E. A., Boroevich, K. A., Inglis, P. N., Li, C., Warner, A., Khattra, J., Holt, R. A., Ou, G., Mah, A. K. et al. (2005). Functional genomics of the cilium, a sensory organelle. *Curr. Biol.* **15**, 935-941.

Broadhead, R., Dawe, H. R., Farr, H., Griffiths, S., Hart, S. R., Portman, N., Shaw, M. K., Ginger, M. L., Gaskell, S. J., McKean, P. G. et al. (2006). Flagellar motility is required for the viability of the bloodstream trypanosome. *Nature* **440**, 224-227.

Castleman, V. H., Romio, L., Chodhari, R., Hirst, R. A., de Castro, S. C., Parker, K. A., Ybot-Gonzalez, P., Emes, R. D., Wilson, S. W., Wallis, C. et al. (2009). Mutations in radial spoke head protein genes RSPH9 and RSPH4A cause primary ciliary dyskinesia with central-microtubular-pair abnormalities. *Am. J. Hum. Genet.* **84**, 197-209.

Chilvers, M. A. and O'Callaghan, C. (2000). Analysis of ciliary beat pattern and beat frequency using digital high speed imaging: comparison with the photomultiplier and photodiode methods. *Thorax* **55**, 314-317.

Chodobski, A. and Szmydynger-Chodobska, J. (2001). Choroid plexus: target for polypeptides and site of their synthesis. *Microsc. Res. Tech.* **52**, 65-82.

Dawe, H. R., Farr, H. and Gull, K. (2007). Centriole/basal body morphogenesis and migration during ciliogenesis in animal cells. *J. Cell Sci.* **120**, 7-15.

Efimenko, E., Bubb, K., Mak, H. Y., Holzman, T., Leroux, M. R., Ruvkun, G., Thomas, J. H. and Swoboda, P. (2005). Analysis of xbx genes in C. elegans. *Development* **132**, 1923-1934.

Fukatsu, K., Bannai, H., Zhang, S., Nakamura, H., Inoue, T. and Mikoshiba, K. (2004). Lateral diffusion of inositol 1,4,5-trisphosphate receptor type 1 is regulated by actin filaments and 4.1N in neuronal dendrites. *J. Biol. Chem.* **279**, 48976-48982.

Gerdes, J. M., Davis, E. E. and Katsanis, N. (2009). The vertebrate primary cilium in development, homeostasis, and disease. *Cell* **137**, 32-45.

Guirao, B., Meunier, A., Mortaud, S., Aguilar, A., Corsi, J. M., Strehl, L., Hirota, Y., Desoeuvre, A., Boutin, C., Han, Y. G. et al. (2010). Coupling between hydrodynamic forces and planar cell polarity orients mammalian motile cilia. *Nat. Cell Biol.* **12**, 341-350.

Hirokawa, N., Tanaka, Y. and Okada, Y. (2009). Left-right determination: involvement of molecular motor KIF3, cilia, and nodal flow. *Cold Spring Harb. Perspect. Biol.* **1**, a000802.

Huang, da, W., Sherman, B. T. and Lempicki, R. A. (2008). Systematic and integrative analysis of large gene lists using DAVID bioinformatics resources. *Nat. Protoc.* **4**, 44-57.

Ignotz, G. G., Cho, M. Y. and Suarez, S. S. (2007). Annexins are candidate oviductal receptors for bovine sperm surface proteins and thus may serve to hold bovine sperm in the oviductal reservoir. *Biol. Reprod.* **77**, 906-913.

Ishikawa, H., Thompson, J., Yates, J. R., 3rd and Marshall, W. F. (2012). Proteomic analysis of mammalian primary cilia. *Curr. Biol.* **22**, 414-419.

Keller, L. C., Romijn, E. P., Zamora, I., Yates, J. R., 3rd and Marshall, W. F. (2005). Proteomic analysis of isolated chlamydomonas centrioles reveals orthologs of ciliary-disease genes. *Curr. Biol.* **15**, 1090-1098.

Kim, J., Lee, J. E., Heynen-Genel, S., Suyama, E., Ono, K., Lee, K., Ideker, T., Aza-Blanc, P. and Gleeson, J. G. (2010). Functional genomic screen for modulators of ciliogenesis and cilium length. *Nature* **464**, 1048-1051.

Li, J. B., Gerdes, J. M., Haycraft, C. J., Fan, Y., Teslovich, T. M., May-Simera, H., Li, H., Blacque, O. E., Li, L., Leitch, C. C. et al. (2004). Comparative genomics identifies a flagellar and basal body proteome that includes the BBS5 human disease gene. *Cell* **117**, 541-552.

Lim, L., Zhou, H. and Costa, R. H. (1997). The winged helix transcription factor HFH-4 is expressed during choroid plexus epithelial development in the mouse embryo. *Proc. Natl. Acad. Sci. USA* **94**, 3094-3099.

Liu, Q., Tan, G., Levenkova, N., Li, T., Pugh, E. N., Jr, Rux, J. J., Speicher, D. W. and Pierce, E. A. (2007). The proteome of the mouse photoreceptor sensory cilium complex. *Mol. Cell. Proteomics* **6**, 1299-1317.

Madhavi, C. and Jacob, M. (1989). Atypical cilia in the choroid plexus of guineapig. *Indian J. Med. Res.* **90**, 484-489.

Mair, R. G., Gesteland, R. C. and Blank, D. L. (1982). Changes in morphology and physiology of olfactory receptor cilia during development. *Neuroscience* **7**, 3091-3103.

Mayer, U., Küller, A., Daiber, P. C., Neudorf, I., Warnken, U., Schnölzer, M., Frings, S. and Möhrlen, F. (2009). The proteome of rat olfactory sensory cilia. *Proteomics* **9**, 322-334.

Mitchell, S. E., Nogueiras, R., Morris, A., Tovar, S., Grant, C., Cruickshank, M., Rayner, D. V., Dieguez, C. and Williams, L. M. (2009). Leptin receptor gene expression and number in the brain are regulated by leptin level and nutritional status. *J. Physiol.* **587**, 3573-3585.

Nachury, M. V., Seeley, E. S. and Jin, H. (2010). Trafficking to the ciliary membrane: how to get across the periciliary diffusion barrier? *Annu. Rev. Cell Dev. Biol.* **26**, 59-87.

Narita, K., Kawate, T., Kakinuma, N. and Takeda, S. (2010). Multiple primary cilia modulate the fluid transcytosis in choroid plexus epithelium. *Traffic* **11**, 287-301.

Olsen, J. V., de Godoy, L. M., Li, G., Macek, B., Mortensen, P., Pesch, R., Makarov, A., Lange, O., Horning, S. and Mann, M. (2005). Parts per million mass accuracy on an Orbitrap mass spectrometer via lock mass injection into a C-trap. *Mol. Cell. Proteomics* **4**, 2010-2021.

Ostrowski, L. E., Blackburn, K., Radde, K. M., Moyer, M. B., Schlatzer, D. M., Moseley, A. and Boucher, R. C. (2002). A proteomic analysis of human cilia: identification of novel components. *Mol. Cell. Proteomics* **1**, 451-465.

Pazour, G. J., Agrin, N., Leszyk, J. and Witman, G. B. (2005). Proteomic analysis of a eukaryotic cilium. *J. Cell Biol.* **170**, 103-113.

Peters, A., Palay, S. L. and Webster, H. d. (1991). *The Fine Structure Of The Nervous System: Neurons And Their Supporting Cells*. New York: Oxford University Press.

Reboldi, A., Coisne, C., Baumjohann, D., Benvenuto, F., Bottinelli, D., Lira, S., Uccelli, A., Lanzavecchia, A., Engelhardt, B. and Sallusto, F. (2009). C-C chemokine receptor 6-regulated entry of TH-17 cells into the CNS through the choroid plexus is required for the initiation of EAE. *Nat. Immunol.* **10**, 514-523.

Rodrigo, J. P., García-Pedrero, J. M., González, M. V., Fernández, M. P., Suárez, C. and Herrero, A. (2004). Expression of annexin A1 in normal and chronically inflamed nasal mucosa. *Arch. Otolaryngol. Head Neck Surg.* **130**, 211-215.

Roth, Y., Kimhi, Y., Edery, H., Aharonson, E. and Priel, Z. (1985). Ciliary motility in brain ventricular system and trachea of hamsters. *Brain Res.* **330**, 291-297.

Satir, P. and Christensen, S. T. (2007). Overview of structure and function of mammalian cilia. *Annu. Rev. Physiol.* **69**, 377-400.

Sorokin, S. P. (1968). Reconstructions of centriole formation and ciliogenesis in mammalian lungs. *J. Cell Sci.* **3**, 207-230.

Spassky, N., Merkle, F. T., Flames, N., Tramontin, A. D., García-Verdugo, J. M. and Alvarez-Buylla, A. (2005). Adult ependymal cells are postmitotic and are derived from radial glial cells during embryogenesis. *J. Neurosci.* **25**, 10-18.

Stolc, V., Samanta, M. P., Tongprasit, W. and Marshall, W. F. (2005). Genome-wide transcriptional analysis of flagellar regeneration in Chlamydomonas reinhardtii identifies orthologs of ciliary disease genes. *Proc. Natl. Acad. Sci. USA* **102**, 3703-3707.

Suzuki, T., Inoue, I., Yamagata, T., Morita, N., Furuichi, T. and Yamakawa, K. (2008). Sequential expression of Efhc1/myoclonin1 in choroid plexus and ependymal cell cilia. *Biochem. Biophys. Res. Commun.* **367**, 226-233.

Suzuki, T., Miyamoto, H., Nakahari, T., Inoue, I., Suemoto, T., Jiang, B., Hirota, Y., Itohara, S., Saido, T. C., Tsumoto, T. et al. (2009). Efhc1 deficiency causes spontaneous myoclonus and increased seizure susceptibility. *Hum. Mol. Genet.* **18**, 1099-1109.

Takeda, S. and Narita, K. (2012). Structure and function of vertebrate cilia, towards a new taxonomy. *Differentiation* **83**, S4-S11.

Takeda, S., Yonekawa, Y., Tanaka, Y., Okada, Y., Nonaka, S. and Hirokawa, N. (1999). Left-right asymmetry and kinesin superfamily protein KIF3A: new insights in determination of laterality and mesoderm induction by kif3A−/− mice analysis. *J. Cell Biol.* **145**, 825-836.

Tissir, F., Qu, Y., Montcouquiol, M., Zhou, L., Komatsu, K., Shi, D., Fujimori, T., Labeau, J., Tyteca, D., Courtoy, P. et al. (2010). Lack of cadherins Celsr2 and Celsr3 impairs ependymal ciliogenesis, leading to fatal hydrocephalus. *Nat. Neurosci.* **13**, 700-707.

Vladar, E. K. and Stearns, T. (2007). Molecular characterization of centriole assembly in ciliated epithelial cells. *J. Cell Biol.* **178**, 31-42.

Yagi, T. and Kamiya, R. (2000). Vigorous beating of Chlamydomonas axonemes lacking central pair/radial spoke structures in the presence of salts and organic compounds. *Cell Motil. Cytoskeleton* **46**, 190-199.

Zariwala, M., O'Neal, W. K., Noone, P. G., Leigh, M. W., Knowles, M. R. and Ostrowski, L. E. (2004). Investigation of the possible role of a novel gene, DPCD, in primary ciliary dyskinesia. *Am. J. Respir. Cell Mol. Biol.* **30**, 428-434.